electrochem

MDPI

Review

Nanostructure-Based Electrochemical Immunosensors as Diagnostic Tools

Rosaceleste Zumpano, Francesca Polli, Cristine D'Agostino, Riccarda Antiochia, Gabriele Favero and Franco Mazzei *

Department of Chemistry and Drug Technologies, Sapienza University of Rome, P.le Aldo Moro 5, 00185 Rome, Italy; rosaceleste.zumpano@uniroma1.it (R.Z.); francesca.polli@uniroma1.it (F.P.); cristine.dagostino@uniroma1.it (C.D.); riccarda.antiochia@uniroma1.it (R.A.); gabriele.favero@uniroma1.it (G.F.)
* Correspondence: franco.mazzei@uniroma1.it; Tel.: +39-0649913225

Abstract: Electrochemical immunosensors are affinity-based biosensors characterized by several useful features such as specificity, miniaturizability, low cost and simplicity, making them very interesting for many applications in several scientific fields. One of the significant issues in the design of electrochemical immunosensors is to increase the system's sensitivity. Different strategies have been developed, one of the most common is the use of nanostructured materials as electrode materials, nanocarriers, electroactive or electrocatalytic nanotracers because of their abilities in signal amplification and biocompatibility. In this review, we will consider some of the most used nanostructures employed in the development of electrochemical immunosensors (e.g., metallic nanoparticles, graphene, carbon nanotubes) and many other still uncommon nanomaterials. Furthermore, their diagnostic applications in the last decade will be discussed, referring to two relevant issues of present-day: the detection of tumor markers and viruses.

Keywords: electrochemical immunosensor; nanomaterial; diagnostics; tumor biomarker; virus

Citation: Zumpano, R.; Polli, F.; D'Agostino, C.; Antiochia, R.; Favero, G.; Mazzei, F. Nanostructure-Based Electrochemical Immunosensors as Diagnostic Tools. *Electrochem* **2021**, *2*, 10–28. https://doi.org/10.3390/electrochem2010002

Received: 4 December 2020
Accepted: 12 January 2021
Published: 14 January 2021

1. Introduction

Clinical diagnostic is an important area of medicine that includes the detection of disease-related biomarkers, such as metabolites or proteins, in human body fluids [1]. Testing for biomarkers is usually performed in centralized laboratories, requiring well-trained staff, expensive instruments and time-consuming processes [1]. Large automated clinical analyzers based on DNA or protein microarrays are typically employed, including polymerase chain reaction (PCR) and immunoassay methods, such as enzyme-linked immunosorbent assay (ELISA) [2]. In particular, real-time PCR is a promising technology that allows quantitative measurements of multiple genes simultaneously with high sensitivity [2]. Unfortunately, these techniques are expensive, require long times of analysis and are challenging to use at the point-of-care (POC).

Therefore, early diagnostic tests based on sensitive, specific, accurate and, at the same time, fast, cost-effective and POC usable methods are crucial to achieve better-quality health management. Early detection of disease and rapid diagnostics is often the key to success for patient survival. Moreover, accurate monitoring of specific diseases allows early diagnosis, with personalized treatment plans.

Biosensors have been recognized as efficient alternatives to obtain sensitive, fast, cheap, and POC measurements [3]. Among the different types of biosensors, electrochemical immunosensors, based on the transduction of an electrochemical signal generated in the interaction between antibodies and antigens in body fluids, have attracted a lot of attention, due to their high sensitivity, high specificity, accuracy and possibility of miniaturization of the sensing platform; essential requirements for a portable device [4,5]. The use of nanotechnology in immunosensing allowed to enhance biodevices properties; especially miniaturization and sensitivity, thus lowering the detection limits by several orders of

magnitude [6–10]. These results can be reached thanks to the high surface/volume ratio of nanostructured materials by increasing both bioreceptor loading and amplifying the electrochemical signal [11].

Nano-immunosensors have significant applications as diagnostic tools for early diagnosis and management of targeted diseases by facilitating timely therapy decisions and monitoring the disease onset and progression [12,13]. Another feature of the nano-based biosensing devices is their potential wireless link capability, allowing the transmission of data to a global network, where they can be utilized, through suitable artificial intelligence (AI) modeling algorithms, for automated monitoring of the epidemiological situation or for preventing disease outbreaks [14].

This review will discuss nanomaterials' role and antigen-antibody interaction on the electrochemical immunosensor performance. Furthermore, a state of the art of the electrochemical nano-immunosensors for tumor biomarkers detection and virus detection published in the literature in the last decade is also provided.

2. The Role of Nanomaterials in Electrochemical Immunosensors

According to the detection principle employed, the several electrochemical immunodevices reported in the literature are mainly amperometric, impedimetric and field effect transistors (FET)-based immunosensors.

In the case of amperometric and impedimetric immunodevices the electron transfer phenomena is mainly affecting their sensitivity. The increase of the sensitivity can be realized, by promoting the electron transfer (ET) to the transducer or increasing Ab loading onto the electrode surface, with a particular focus on their orientation.

In this context, the use of nanomaterials (NMs) is crucial thanks to their multiple features, such as huge surface area, high conductivity, electro-catalytic and electroactive properties and biocompatibility. NMs can be defined by at least one dimension ranging between 1 and 100 nm. Therefore, they are classified as zero-dimensional (0D), one-dimensional (1D), two-dimensional (2D) and three dimensional (3D) based on how many dimensions they have larger than 100 nm [15]. Important examples are metallic nanoparticles (MeNPs), magnetic nanoparticles (MNPs) and quantum dots (QDs), which belong to the 0D group, and carbon-based nanostructures like fullerene (C60), carbon nanotubes (CNTs), graphene (GN), belonging to 0D, 1D and 2D, respectively.

According to the immunosensor configuration (Figure 1), NMs are mainly employed in the ET enhancement and Ab loading in the case of label-free immunosensors, while in sandwich immunosensors, they can be also used as electroactive or electrocatalytic tracers (non-enzymatic immunosensors) and nanocarriers.

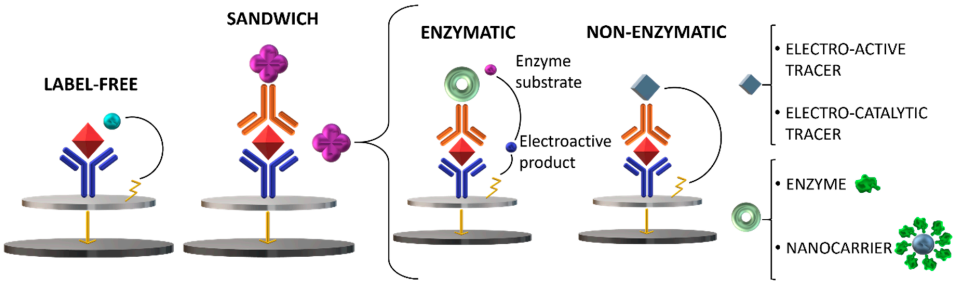

Figure 1. Examples of amperometric immunosensor configurations: the antigen (Ag), primary antibody (Ab) and secondary antibody (Ab_2) are shown in red, blue and orange respectively. The Ab_2 generic label is shown in violet.

2.1. Metallic Nanoparticles

Metallic nanoparticles (MeNPs) are suitable electrode materials, improving ET and promoting the immobilization of a significant number of Ab molecules, thanks to their high surface energy, large surface area, high conductivity, electrocatalytic/electroactive properties and biocompatibility.

There are several ways of achieving antibody-MeNP bioconjugation, divided into physical and chemical methods [16]. The physical methods are mainly based on: (i) the spontaneous adsorption of the Ab onto the MeNP surface through the hydrophobic interaction between the Ab lipophilic parts and the MeNP surface; (ii) the electrostatic attraction between the MeNP and the Ab [17] (Figure 2a).

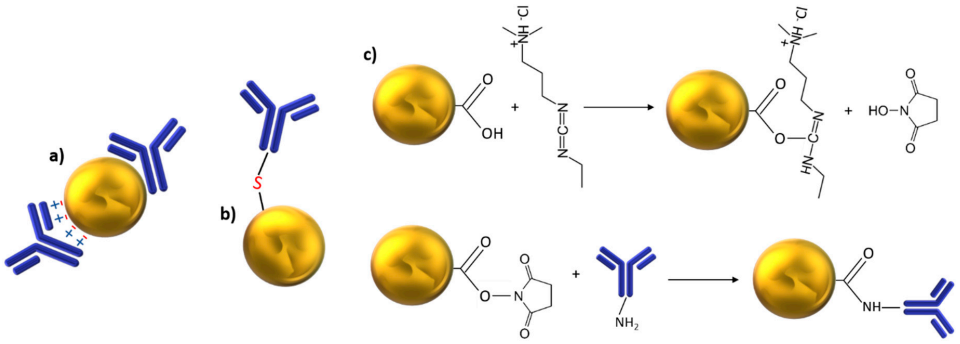

Figure 2. Ab–AuNPs bioconjugation mechanisms: (**a**) hydrophobic and electrostatic interactions; (**b**) Au-S dative bond; (**c**) EDC/NHS chemistry.

In the case of chemical methods, several covalent strategies have been realized. The most common way is based on the binding of the Ab directly to the MeNPs surface via its thiol-groups (Figure 2b) [18]. Another method is based on the functionalization of the MeNPs with bifunctional linkers (carboxyl-thiols, amine-thiols) or adapter molecules (streptavidin, biotin) and making them react with the Ab via EDC/NHS chemistry (Figure 2c) [16,19]. Several works employing Au, Pt, Pd, Cu, Ag nanoparticles as electrode materials are found in the literature [20–29]. However, despite their numerous features, MeNPs are not suitable for sufficient signal amplification by themselves [30]. For this reason, they are used combined with other nanostructures, such as GN, CNTs, C_{60}, conductive polymers, obtaining remarkable synergistic effects [31].

For instance, in 2019 Fan et al. [20] realized a paper-based immunosensor for the detection of cancer antigen 125 (CA125), by modifying the working electrode with reduced GN/thionine/AuNPs nanocomposites where anti-CA125 was immobilized. GN's nanoporous structure combined with AuNPs provided a significant signal enhancement with a limit of detection (LOD) of 0.01 U mL^{-1}.

Moreover, in 2020 Suresh et al. [23] developed a sandwich-type enzymatic immunosensor to detect prostate cancer. A nanocomposite film constituted by polyaniline (PANI), C_{60} and PtNPs was used to modify the glassy carbon (GC) electrode surface, allowing the Ab immobilization. After incubation with the prostate-specific antigen (PSA) and the Ab_2 marked with horseradish peroxidase, the H_2O_2 reduction signal was significantly enhanced, with a LOD for PSA of 1.95×10^{-5} ng mL^{-1}. The MeNPs size plays an essential role in the ET efficiency and in 1995 Doron et al. developed an interesting proof-of-concept study [32]. They prepared AuNPs films on indium tin oxide (ITO) surfaces functionalized with (aminopropyl)siloxane or (mercaptopropyl)siloxane. Different sizes of AuNPs were used in the range between 25 nm and 120 nm. They saw that smaller nanoparticles gave better surface coverage and more homogeneous films than the bigger ones. This result was reflected in the voltammetric response of a redox mediator, 8-(*N*-methyl-4,4′-bipyridinyl)octanoic acid, covalently linked to a cystamine monolayer formed onto the AuNPs films. The bigger the AuNPs size, the lower the current intensity.

Very interesting is the Me/multiMeNPs application as electroactive or electrocatalytic labels in sandwich-type immunosensors. In particular, multiMeNPs, compared to single metals, show higher electrocatalytic performances thanks to unique electronic effects between all the metals forming the alloy [33]. Several works report examples of Me/multiMeNPs used as Ab_2 markers to catalyze the production of electroactive species or their reaction at the electrode [34–36]. AuNPs are also known to catalyze the reduction

of Ag^+ ions onto their surface. Through the Ag^0 re-oxidation a signal related to the AuNPs number, thus to the Ab_2 molecule number, is produced [37]. Other works show MeNPs markers acting as electroactive species by themselves. It is known that strong acidic conditions induce the Au and Ag oxidation, especially if present in their colloidal form. The subsequent Au^+ and Ag^+ reduction by the electrode produces a current intensity related to the target concentration [38–40]. Despite the high sensitivity reached in this case, the time required for the dissolution-step and the strong acidic conditions by themselves are important issues to take into account.

MeNPs are often employed to realize nanocarriers, binding a large number of enzyme molecules or redox probes; once the nanocarrier is labeled to the Ab_2 it amplifies the signal drastically [41,42]. Finally, MeNPs-coupled with MNPs, metal-covered MNPs, and QDs deserve to be mentioned as having unique and incredible properties. MeNPs-coupled or metal-covered MNPs, by using an external magnet, promote an efficient Ab immobilization and easy sample washing procedure after incubation [43,44]. QDs are core-shell NPs made of semiconductor metals. Common metals employed in the QDs realization are Pb, Zn and Cd, easy to detect electrochemically. By using different QDs in the same immunosensor, multidetection systems were realized [45].

2.2. Carbon-Based Nanomaterials (NMs)

In the past few decades, carbon-based NMs (CNMs) found an extensive application in the electrochemical biosensors field of research. They are composed of carbon atoms sp^2 hybridized, offering a wide variety of nanostructure morphologies (Figure 3). Indeed, carbon displays several well known allotropic forms, such as diamond, α and β graphite (GPH), fullerenes, nanotubes, with peculiar features depending on their shape.

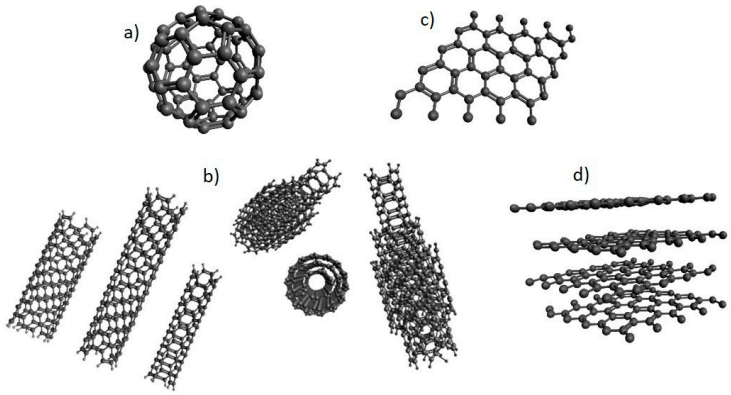

Figure 3. Examples of carbon-based nanostructures: (**a**) fullerene 0D; (**b**) SWCNTs and MWCNTs 1D; (**c**) GN 2D; (**d**) GPH 3D.

They all show high surface area, electrocatalytic and mechanical properties, chemical stability, high conductivity and biocompatibility [46], making them suitable as electrode materials, electrocatalytic tracers and nanocarriers. Moreover, CNMs have always been appreciated for their intriguing electronic properties comparable to those of metals and semiconductors, as much as for their easy synthesis and functionalization via several approaches [47].

The youngest, in terms of its synthesis discovery in 2004, is GN. It represents the basic building block to form fullerenes, GPH, and CNTs [48]. Given its planar geometry, most surface atoms are exposed, allowing the binding of a high number of Ab molecules. To solubilize the GN in aqueous media a pre-functionalization with groups such as –COOH is required [30]. For this purpose, GN oxide (GO) finds broader applications, also due to its facile synthesis via GPH oxide exfoliation providing a more defective product. Indeed, it is demonstrated that more structural defects improve the electrochemical properties of GN [49]. However, the GN oxidation induces the distortion of the sp^2 hybridization with the consequence of an insulating system. For these reasons, the reduction

step is crucial to obtain the GO reducted form (rGO) and restore the conductive properties [50]. Several works employing GN and rGO as electrode materials are present in the literature [51–58]. Almost all show the additional presence of MeNPs, resulting in MeNPs decorated–GN/rGO systems with incredibly high catalytic and conductive properties. For instance, Wang et al. in 2018, realized a label-free immunosensor for carcinoembryonic antigen detection (CEA). They modified a GC electrode with AgPt nanorings–rGO, where the Ab was then physically immobilized. They obtained a highly sensitive sensor, with a LOD for CEA of 1.43 fg mL^{-1}.

GN is also employed as a nanocarrier in sandwich-type electrochemical immunosensors [59,60]. In this regard, GN quantum dots (GQDs), formed by small pieces of GN shorter than 100 nm, deserved to be mentioned. Thanks to the presence of numerous edge defects and quantum confinement, they show high catalytic properties and facile bioconjugation, besides all the other GN properties [61]. For this reason, one can find several works in literature where GQDs are used as nanocarriers and electrocatalytic tracers [62,63]. GQDs, together with carbon nanodots (CNDs) and carbon quantum dots (CQDs) belong to the more general carbon nanoparticles (CNPs) family. CQDs and CNDs differ because the first has a crystalline structure that involves quantum confinement, whereas the latter are amorphous with no quantum confinement. Overall, CNPs have incredible features such as high porosity, good conductivity, high surface area and electrocatalytic activity, which make them ideal for Ab immobilization, ET enhancement and Ab_2 labeling [64]. Moreover, the use of GO nanocolloids (GONCs), both as immobilization platforms and electroactive tracers, proved to be of great interest in this context [65].

As reported above, GN is the building block for other C allotropic forms, such as CNTs. CNTs have always enjoyed great interest, since many years before GN. They are single-walled (SW) or multi-walled (MW) with a diameter comparable to the size of a single protein (e.g., 1 nm in the case of DNA), and several micrometers long [66]. Hence, in addition to their natural biocompatibility, they also result size-compatible with biomolecules. Moreover, they show great flexibility, chemical stability, large surface area, and particular electronic properties [67]. Indeed, considering SWCNTs as a rolled GN sheet forming a cylinder, the π-π^* system undergoes a distortion which induces a partial σ-π hybridization. Their electronic properties strongly depend on the diameter and chirality [50]. Easy to functionalize with –COOH groups via oxidation with HNO_3, or with $–NH_2$ groups via amination, CNTs are excellent electrode materials [68–72] and nanocarriers [73,74]. However, CNTs show some disadvantages compared to GN. Their synthesis is made via MeNPs catalysis, which induces the presence of MeNPs residues in the final product. This factor leads to some problems: metallic residues, if present, can dominate the CNTs electrochemistry and, worse still, they may pose toxicological hazards [75]. Carbon nanohorns (CNHs) are a particular metal-free form of CNTs, with a cone structure.

Specifically, CNHs have a high defective structure which makes them easy to functionalize and to employ in the realization of several composites with other nanomaterials such as MeNPs, alloys, fullerenes, CNPs [61]. Until 2010, not many electrochemical immunosensors based on CNHs were reported. During the last ten years, they have been employed both as electrode materials [76–79] and as electrocatalytic tracers/nanocarriers [40,80,81].

Great importance is given to fullerenes, in particular C_{60}, which is the smallest existing stable one. Differently from other allotropic forms, fullerenes are formed by pentagonal and hexagonal rings, sp^2 hybridized. Double bonds are present only in hexagonal rings, and for this reason, C_{60} has not the same π delocalization as the other allotropes and shows electron-deficiency. This feature makes fullerenes highly reactive towards electron-rich species, behaving as an electron-poor alkene [82]. Moreover, fullerene functionalization is very simple via cycloaddition, nucleophilic or radical addition [83], as well as their decoration with other nanostructures (e.g., MeNPs). Several works are present in the literature involving fullerenes as electrode materials and labels, acting as good Ab immobilizers and ET enhancers [84–87].

Lastly, nanodiamonds (NDs) deserve to be mentioned. They are uncommon compared to the other CNMs, probably because of their difficult synthesis and, therefore, high costs. However, NDs are very promising for electrochemical immunosensor development, thanks to their high chemical and physical stability, large surface area, and facile functionalization [50], making them good Ab immobilizers [88].

3. Nano-Immunosensors for Tumor Biomarkers Detection

An electrochemical immunosensor represents an excellent opportunity to create a device for the detection and quantification of tumor markers by exploiting the technique's advantages: high sensitivity, reduced testing time and costs compared to classical diagnostic methods. It is thus potentially possible to perform analytical tests outside the facilities of the clinical reference laboratory, also reducing the time of execution and response of analytical tests (POCT-point of care testing) [89,90]. The measurement of single tumor antigens can often lead to false positives or false negatives [91]. However, accurate quantification, especially simultaneous monitoring of multiple tumor antigens, can facilitate an earlier screening of a small tumor and an easier diagnosis [92,93]. In the last ten years, the electrochemical goal has therefore been the realization of detection/quantification systems for the most widespread and important tumor markers including carcinoma antigen CA (CA125, CA15-3, CA19-9, CA242), prostate-specific antigen (PSA), carcinoembryonic antigen (CEA), α-fetoprotein (AFP) and cytokeratin 19 fragment 211 (CYFRA211) [94].

3.1. Mucin Associated Antigens as Tumor Markers: Metallic Nanoparticles/Carbon Nanostructured Based-Electrochemical Immunosensors

Mucins are glycoproteins with high molecular weight (>50 kD), high carbohydrate content (50–80%) characterized by the presence of O-glycosidic bonds and having high density and viscosity. They are usually found on the surface of the epithelia and represent the significant constituent of mucous membranes.

Characterized by repetitive sequences of serine and/or threonine and proline, they can be found in circulation at low concentrations under normal conditions, but their level increases during the proliferation of neoplasms. For this reason, they are used as prognostic indicators for lots of cancers even if they are not considered specific to an organ instead associated with a particular type of neoplasia [95–97]. Many of electrochemical immunosensors to detect cancer antigens CA use metallic nanoparticles as an electrode material because of their excellent electron transfer capacity [98]. For instance, in 2018 Kumar, Sharma and Nara reported a dual gold nanostructure-based electrochemical immunosensor to detect ovarian cancer biomarker carcinoma antigen 125 (CA125) in serum with a detection limit of 3.4 U/mL and a linear range of 20–100 U/mL (CA125 cut off value 35 U/mL [99]) [100]. They used gold nanorods (AuNRs) covered indium tin oxide (ITO) as the working electrode after immobilizing capture anti-CA125 on it. AuNPs were used as a probe immobilizing another anti-CA125 antibody tagged with metal ion Cd^{2+}. The format is sandwich-type with the antigen between the two antibodies, and the detection is obtained in differential pulse voltammetry by the cadmium characteristic peak, which corresponds to CA125 concentration.

Even more recently, Pakchin and his colleagues have developed a novel electrochemical immunosensor for the ultrasensitive detection of CA125 (LOD around 6 μU/mL) performing a linear range 0.0005–75 U/mL [101]. AuNPs have been used again but this time combined with polyamidoamine (PAMAM) dendrimer to increase the conductivity and provide functional groups to covalently conjugate anti-CA125 antibodies on the electrode surface. They used as a platform a GC electrode modified with three-dimensional rGO-MWCNTs to improve both the specific area and the electron transfer. The label was made up of O-succinyl-chitosan-magnetic nanoparticles (Suc-CS@MNPs) with the antibody and toluidine blue (TB) attached on. The format is again sandwich-type and the detection is by voltammetry. Therefore, these two electrochemical immunosensors represent interesting methods for monitoring the carcinoma antigen 125 with an excellent LOD, improving the prognostic stratification of patients with endometrial carcinoma (EC) [102].

Based on the immunosensor configuration (label-free or sandwich enzymatic/non-enzymatic), it is possible to make different sensitive platforms. Huang et al. developed a simple label-free electrochemical immunoassay for the biomarker carbohydrate antigen 19-9 (CA19-9) based on polythionine-Au composites (AuNPs@PThi) as a probe [103]. CA19-9 is the most indicated tumor marker in tumors of the pancreas, liver, stomach and colon and has a high prognostic value since a rapid reduction in levels following surgical therapy correlates with a good degree of resection of active neoplasia. In the configuration reported by Huang the anti-CA19-9 was simply dropped on a GC electrode modified with AuNPs cross-linked by the AuNPs@PThi agent. Different concentrations of CA19-9 caused electrochemical responses depending on the electron transfer blocked after the immunoreaction; the peak currents in DPV measurement decreased while increasing the CA19-9 concentration. The immunosensor works in a range from 6.5 to 520 U/mL (CA19-9 cut off value 37 U/mL [104]) with a LOD of 0.26 U/mL. Once again, the use of nanoparticles not only involves signal amplification but also allows high sensitivity, excellent LOD, stability and reproducibility.

Not only metallic nanoparticles, but also carbon-based structures can be used in diagnostics to achieve these goals. For example, in 2017 Armani et al. developed an electrochemical immunosensor for the breast cancer marker CA15-3 based on the catalytic activity of CuS/rGO nanocomposite towards the electrooxidation of catechol [51]. The cut-off of this tumor marker is 30 U/mL [105] and they have reached a great LOD of 0.3 U/mL with a linear working range 1.0–150 U/mL. The use of GN as a support matrix for CuS has proven to be extremely convenient because of its good electronic conductivity and its large surface area, resulting in excellent performance.

Ge et al., some years earlier, achieved a far better detection limit of 5 μU/mL with a slightly more complicated system, with a linear working range of 2×10^{-5}–40 U/mL [106]. They used thionine (TH)-nanoporous gold (NPG)-GN labeled primary antibody as the electrodic platform and horseradish peroxidase (HRP)-encapsulated liposomes labeled secondary antibodies as labels. The format is sandwich-type with the CA15-3 antigen stuck between HRP@liposomes and TH-NPG-GN. The benefits in the use of NPG are its high surface area, very high conductivity and excellent stability.

Different applications also concern the use of multimetallic nanocomposites that involve high catalytic ability and large surface/volume ratio. An example is the one reported by Xi Du et al. concerning a label-free electrochemical immunosensor for detection of the tumor marker CA242 (cut-off 20 U/mL [107]) investigated in pancreatic and colorectal cancers [108], the first one based on the redox-active rGO-Au-Pd nanocomposite. This immunosensor exhibits a linear range of 0.001–10,000 U/mL with a LOD of 1.54×10^{-3} U/mL and it could be used in early diagnosis. An alternative is the use of a hydrogel-based immunosensor, a three-dimensional porous material composed by interpenetrating polymer networks (IPNs), characterized by large surface area, excellent hydrophilicity and biocompatibility [109]. Tang et al. have coated a GC electrode with a sodium alginate-Pb^{2+}-GO (SA-Pb^{2+}-GO) hydrogel to detect CA242 [110]. First, they covered the gel with chitosan-Pb^{2+} to improve conductivity and then immobilized the anti-CA242. CA242 detection promotes an increase of the resistance causing a drop in current. This ultrasensitive label-free immunosensor exhibits an excellent LOD of 0.067 mU/mL and a linear range of 0.005–500 U/mL.

3.2. Oncofetal Proteins as Tumor Markers: Carbon-Based Nanostructures, Nanodots and Nanocages in Electrochemical Immunosensors

Oncofetal proteins are normally present during embryogenesis but their level can increase as a degradation product of tumor cells thus becoming extremely useful tumor markers for a precocious diagnosis. There are several examples of electrochemical immunosensors used for clinical diagnosis of the most common oncofetal antigens such as carcinoembryonic antigen (CEA) and α-fetoprotein (AFP). CEA is a tumor marker usually present in human serum (2.5–5 ng/mL) [111] and over-expressed when colon carcinomas, pancreas, liver, lung and ovarian cancer occur [112]. Recently Idris et al. have developed a

new platform based on nanocomposite of polypropylene imine dendrimer (PPI) and carbon nanodots (CNDTs) on an exfoliated GPH electrode (EGE) for the detection of CEA [113]. CNDTs and PPI properties of chemical stability, excellent biocompatibility and high surface area allowed a label-free electrochemical immunosensor with the direct immobilization of the anti-CEA on the nanocomposite platform. Measurements were carried out in a $[Fe(CN)_6]^{3-/4-}$ solution by DPV in a concentration range of 0.005–300 ng/mL, obtaining a low LOD of 0.00145 ng/mL, good reproducibility and selectivity. Li and coworkers have developed an even more sensitive immunosensor using MWCNT-NH_2 supported PdPt nanocages as labels of the secondary anti-CEA [114]. First a GC electrode was modified with 3-aminopropyltriethoxysilane GN sheets (GS) to enhance the electron transfer and then the primary antibody was immobilized. The electrochemical immunosensor is sandwich-type and the detection is made through the reduction of H_2O_2. It exhibits a linear range from 0.001 to 20 ng/mL with an ultra LOD of 0.2 pg/mL for CEA. AFP is a glycoprotein produced by the fetal liver and yolk sac during the first few months of gestation and its concentration is typically high at birth and then decreases rapidly [115]. Liver damage and some tumors (hepatocellular carcinoma, hepatoblastoma, testicular and ovarian cancer) can significantly increase AFP concentration, which makes the protein useful as a tumor marker. It is crucial to make an early diagnosis, so several electrochemical immunosensors have been developed to break down testing times, measurement difficulties, and high costs. For example, in 2016 Jiao developed an immunosensor with an ultralow LOD of 0.05 pg/mL and a linear range within 0.1 and 10 ng/mL [116]. The developed sandwich-type electrochemical immunosensor for AFP is based on amino group GS loaded mesoporous Au@Pt nanodendrites (NH_2-GS-Au@Pt) as label and a GC electrode modified with poly-dopamine (PDA) N-doped functionalized MWCNTs (PDA-N-MWCNTs) as platform. PDA-N-MWCNTs show good biocompatibility for the immobilization of the primary antibody and make the electrode with a higher surface area whereas bimetallic Au@Pt nanodendrites exhibit an excellent electrocatalytic activity; both contribute to increase the sensitivity of the system. Liu et al. have recently proposed a strategy for a sensitive label-free electrochemical immunosensing platform based on aligned gallium nitride (GaN) nanowire array characterized by excellent biocompatibility and chemical stability, with high surface/volume ratio and electron mobility [117]. PDA was self-assembled on GaN nanowires and then the GaN-PDA hybrid modified with AuNPs linked the anti-AFP. The dynamic range (0.01 to 100 ng/mL) was evaluated by DPV, showing a LOD down to 0.003 ng/mL.

4. Nano-Immunosensors for Virus Detection

Viral infections pose a serious threat to public health and the global economy. Therefore, a rapid and accurate diagnosis can mean the difference between the resolution of the epidemic and the uncontrolled spread with a serious threat to the survival of individuals and companies. Currently, the most adopted methods for the diagnosis of viral infection involves the use of specialized laboratories, sophisticated tools and technologies not available in many areas of the world, and times ranging from 6 to 24 h. To speed up diagnoses, point-of-care (POC) tests are necessary.

It has already been mentioned that POCTs involves rapid diagnostic tests carried out at the site of patient care [118,119]. As far as the virus detection is concerned, it should be pointed out that the fundamental concept of the POC is to carry out the test most comfortably and immediately for the patient, who can hand-hold and carry out the test, obtain immediate medical reports and receive the first treatment directly at home, without having the discomfort to go to centralized hospitals or specialized health centers, thus avoiding the risk of contracting or transmitting infectious diseases, in the case, for example, of viral pathogens. To obtain enhanced sensitivity biodevices, in the last years, nanotechnology materials were extensively used in the development of electrochemical modified immunosensors for virus detection [120–122]. Below we will describe examples of electrochemical immunosensors, realized using nanoparticles of various types (Table 1).

Table 1. Most relevant examples of nanostrustured-based electrochemical immunosensors as a diagnostic tool (see below for abbreviations).

Target Antigen	Electrode Configuration	Label	Detection	LOD	Linear Range	Ref.
CA125	Ab/rGO/Thi/AuNPs/GC	Label-free	DPV	0.01 U/mL	0.1–200 U/mL	[20]
	Ab/AuNPs-PB-PtNP-PANI/GC	Label-free	SWV	4.4 mU/mL	0.01–5000 U/mL	[24]
	ITO-AuNRs-Ab	AuNPs-Ab-Ca^{2+}	DPV	3.4 U/mL	20–100 U/mL	[100]
	Ab-3DrGO-MWCNTs-PAMAM/AuNPs-GC	Ab-Suc-CS@MNPs-TB	SWV	6 µU/mL	0.0005–75 U/mL	[101]
CA19-9	Ab-AuNPs/AuNPs@PThi/GC	Label-free	DPV	0.26 U/mL	6.5–520 U/mL	[103]
CA15-3	CuS-rGO/Ab	Label-free	DPV	0.3 U/mL	1.0–150 U/mL	[51]
	Ab/TH-NPG-GN/GC	HRP@liposomes/Ab_2	DPV	5 µU/mL	2×10^{-5}–40 U/mL	[106]
CA242	rGO-Au-Pd-Ab/GC	Label-free	DPV	0.00154 mU/mL	0.001–10,000 U/mL	[108]
	Ab/Chit-Pb^{2+}-/SA-Pb^{2+}-GO/GC	Label-free	SWV	0.067 mU/mL	0.005–500 U/mL	[110]
CEA	Ab-biotin-streptavidin-PtNPs@rGO@PSNSs/GC	Label-free	DPV	0.01 ng/mL	0.05–70 ng/mL	[25]
	Ab/AuNPs/NB-ERGO	Label-free	DPV	0.00045 ng/mL	0.001–40 ng/mL	[53]
	Ab/AgPt NRs-rGO	Label-free	EIS	1.43 fg/mL	5 fg/mL–50 ng/mL	[56]
	Ab/rGO-AuNPs/GC	SWCNTs@GQDs/Ab_2	EIS, CV	5.3 pg/mL	50–650 pg/mL	[63]
	Ab/AuNPs-MWCNTs-Chits/GC	Label-free	DPV	0.01 ng/mL	0.3–20 ng/mL	[70]
	EG/CNDTs@PPI/Ab	Label-free	DPV	0.00145 ng/mL	0.005–300 ng/mL	[113]
	Ab/NH_2-GS/GC	PdPt nanocages/MWCNTs-NH_2-Ab_2	CA	0.2 pg/mL	0.001–20 ng/mL	[114]
AFP	ADA-Ab/CD-GS	PdNi/N-GNRs-Ab_2	CV	0.03 pg/mL	0.0001–16 ng/mL	[35]
	PDA-N-MWCNTs/GC	NH_2-GS-Au@Pt	EIS	0.05 pg/mL	0.1–10 ng/mL	[116]
	Ab/AuNPs/PDA/GaN nanowires	Label-free	DPV	0.003 ng/mL	0.01–100 ng/mL	[117]
PSA	Ab/PdNP@PANI-C60/GC	HRP-Ab_2	DPV	1.95×10^{-5} ng/mL	1.6×10^{-4}–38 ng/mL	[23]
	Ab/HQ@CuNPs-reduced-fullerene-C60/GC	HRP-Ab_2	DPV	0.002 ng/mL	0.005–20 ng/mL	[27]

Table 1. *Cont.*

Target Antigen	Electrode Configuration	Label	Detection	LOD	Linear Range	Ref.
	Ab/AuNPS/rGO/Au	Label-free	DPV	3 pg/mL	6 pg/mL–30 ng/mL	[52]
HBV	HBsAb-MNPs	Ab_2AuNPs/hemin/ G-Quadruplex/MB	SWV	0.19 pg/mL	0.3–1000 pg/mL	[42]
	HRP-Ab–AuNPs/DTSP/NPG	HRP	DPV	2.3 pg/mL	0.01–0.1ng/mL	[123]
	HBsAb-MNPs	HBsAb-AuNPs/Cu	ASW	87 pg/mL	0.1–1500 ng/mL	[124]
	GO/Fe_3O_4/ PB@AuNPs/SPE	Label-free	CV	0.16 pg/mL	0.5–200 ng/mL	[125]
CoV	Au/MNPs	Label-free	SWV	0.1 pg/mL	0.001–100 ng/mL	[126]
	Ab-PBASE/GN	Label free	FET	2.42×10^2 cp/mL	-	[120]
	$anti_m$IgG-Ab-MNPs	$anti_r$IgG-Ab_2-AP	DPV	19 ng/mL (S) 8 ng/mL (N)	-	[121]
H1N1	Ab/RGO/Au	Label-free	CA	0.5 pfu/mL	1–104 pfu/mL	[54]
HIV	MNPs-Ab	AuNPs/Ac-HRP-Ab_2	DPV	0.5 pg/mL	0.001–10.00 ng/mL	[122]

CA—Carbohydrate Antigen; CEA—Carcinoembryonic Antigen; AFP—Alpha Fetoprotein; PSA—Prostate Specific Antigen; HBV—Hepatitis B Virus; CoV—Human Coronavirus; H1N1—Influenza A; HIV—Human Immunodeficency Virus; GC—Glassy Carbon; ITO—Indium Tin Oxide; AuNRs—Gold Nanorods; AuNPs—Gold Nanoparticles; Ab—Antibody; GO—Graphene Oxide; rGO—Reduced Graphene Oxide; SWCNTs—Single Walled Carbon Nanotubes; MWCNTs—Multi Walled Carbon Nanotubes; CNTs—Carbon Nanotubes; PAMAM—Poly(amidoamine); MNPs—Magnetic Nanoparticles; PANI—Polyaniline; NPG—Nanoporous Gold; HRP—Horseradish Peroxidase; PDA—Poly-Dopamine; PB—Prussian Blue; TB—Toluidine Blue; Chit—Chitosan; DTSP—Dithiobis(succinimidyl propionate); GN—graphene.

4.1. HBV (Hepatitis B Virus)

Nanoparticles are widely used in the development of immunosensors for the HBV virus, whose early diagnosis is based on the detection of the viral surface antigen HBsAg (human B surface antigen). For this purpose, in 2010, Ding et al. developed a sandwich immunosensor, where the antigen capture interacts with HRP-labeled antibodies immobilized on AuNPs (Figure 4). To enhance the surface area suitable for the electron transfer, a nanoporous gold electrode (NPG) was utilized. Once the immunocomplex is formed, in the presence of H_2O_2, HRP oxidize the mediator OPD (*o*-phenylenediamine) giving the cathodic peak required for the calibration of the sensor [123]. In this work, the advantages of using the NPG electrode are combined with the signal amplification provided by AuNPs, leading to an increase in the sandwich method's sensitivity.

Figure 4. HBV sensor for the detection of HBsAg with HRP/Ab-AuNPs.

A few years later, Alizadeh et al. used two different types of nanoparticles in their work, exploiting the biocompatibility and the ability to increase the antibody loading of Fe_3O_4 nanoparticles and the signal amplification connected to the use of gold ones. In this instance, AuNPs play a structural role by representing the core of a DNAzyme, a mimetic analog of HRP characterized by high stability and high catalytic activity [42]. For this purpose, the AuNPs have been conjugated with hemin/G-quadruplets, a complex able to substitute the HRP electrochemical catalysis of methylene blue in the presence of H_2O_2 [127]. The HBsAg is therefore bound at the same time to the primary antibody-carried by magnetic nanoparticle-and to the secondary antibody of the DNAzyme, responsible for the electrochemical signal. This method shows a LOD of 0.19 pg/mL.

Moreover, the 3-component immunocomplex can be easily separated by taking advantage of the superparamagnetic characteristics of the Fe_3O_4 nanoparticles, as presented in the work of Zhang et al. [124]. After the magnetic separation, the complex is prepared for the copper enhancement during which the Cu^{2+} ions are reduced by ascorbic acid all around AuNPs (Figure 5). The metal is then released by strong acid dissolution and the Cu^{2+} ions are measured by anodic stripping voltammetry (ASV) applying a deposition potential of −0.5V (versus SCE) for 7 min.

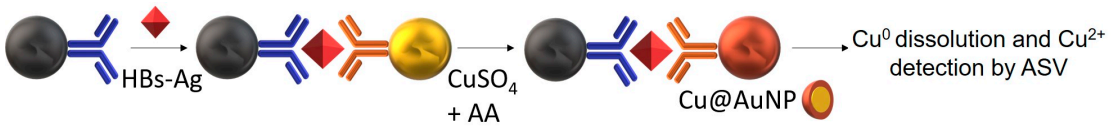

Figure 5. HBV sensor with copper enhanced technique. MNPs, AuNPs and the copper shell are shown in grey, yellow and red, respectively.

Another advantage of this method is the usage of a copper-enhancer solution, easy to prepare and preserve when compared with other common metal enhancers (e.g., silver or gold) [128]. An example of a label-free immunosensor, is given by the work of Wei et al. in which the nanostructure ($GO/Fe_3O_4/PB$) plays a role not only as electrode material but also as a redox probe. (GO/Fe_3O_4) is dropped onto the electrode, while PB and AuNPs are generated in situ. AuNPs are prepared by electrodeposition from HAuCl4 to enhance the

detection sensitivity. After the immobilization of HBsAg antibodies, the electrochemical signal is given by Prussian Blue, whose signal decrease is proportional to the amount of antigen bound to the sensor [125].

4.2. CoVs (Human Coronaviruses)

The contagious nature and the high clinical significance stimulated the development of advanced detection methods for coronaviruses like Middle East Respiratory Syndrome (MERS) and Severe Acute Respiratory Syndrome (SARS). These are characterized by high contagiousness and high mortality due to their ability to cause severe pneumonia [129]. To date, the diagnosis of these viruses is performed by PCR, a molecular test characterized by high costs and time analysis. These factors are reduced by switching to serological tests to detect the presence of antibodies in the host serum. However, they suffer from low sensitivity and problems related to antibody response latency.

Within assays based on antibody-antigen binding, in 2019, Lailaq and Eissa designed a high-sensitivity immunosensor for the detection of the S1 viral antigen (Spike protein), rather than the antibody response [126]. In their work, they used a competitive immunoassay, immobilizing the recombinant antigen on the chip and letting it interact for 20 min with a solution obtained by mixing a set amount of antibody together with the antigen sample. To increase the electron transfer rate and increases the electrode area, which improves the biosensor response signal, the carbon electrode was modified with AuNPs. The electrochemical signal is detected by square wave voltammetry (SWV) recording the changes in peak current of the probe ferrocyanide/ferricyanide due to the addition of different concentrations of S1. The sensor exhibits a LOD of 1.0 pg/mL for MERS-CoV and shows a high selectivity over other viruses' proteins (e.g., Influenza A and B).

Around the same time, Seo and Lee developed a FET for the detection of SARS-CoV-2, the strain responsible for the disease COVID-19 [120]. Here, GN is used as a sensing material due to its high electronic conductivity and carrier mobility. To immobilize spike protein antibodies on GN, 1-pyrenebutyric acid N-hydroxysuccinimide ester (PBASE) is used thanks to its ability to form amide bonds with lysine residues of the antibody and π-π^* stacking interaction with GN (Figure 6). The sensor was also tested in clinical samples and a LOD of 2.42×10^2 viral copies/mL was achieved. A highly sensitive electrochemical immunosensor was developed by Fabiani et al. allowing a rapid and non-invasive detection of the SARS-Cov-2 Spike protein (S) and nucleocapsid (N) in untreated saliva [121]. In their sandwich immunoassay, the secondary antibody was labelled with alkaline phosphatase (AP) to detect the signal of 1-naphthol while the capture one was linked on the surface of magnetic nanoparticles. This sensor has shown a detection limit of 19 ng/mL and 8 ng/mL for S and N proteins, respectively.

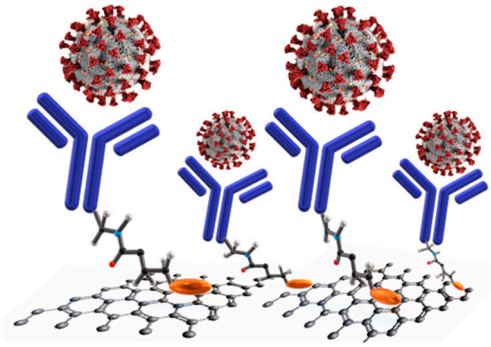

Figure 6. Scheme of SARS Cov-2 FET sensors with the PBASE pyrene conjugated system in orange.

4.3. H1N1 (Influenza A)

The H1N1 virus is a pathogen able to cause acute symptoms of a respiratory infection such as high fever, lethargy, and coughing in the host. In February 2010 it was responsible

for about 16,000 deaths, according to the World Health Organization. To date, the diagnostic method uses both immunological and molecular assays (e.g., PCR).

An electrochemical immunosensor for label-free detection of influenza virus is reported in 2017 by Singh et al. who developed a microfluidic chip GO-based, extremely suitable for minute samples [54]. rGO is a widely used nanostructure in biosensors with a good biocompatibility and conductivity. The chip consists of an integrated microfluidic electrochemical immunosensor in which the gold working electrode is modified with cysteamine (CA) and then with rGO whose carboxyl groups are conjugated with antibodies through EDC/NHS coupling. Due to high conductivity, large surface area, and electron transport properties, modification with rGO accelerates electron transfer rate and improves redox conversion at the electrode/electrolyte interface, leading to an increase in the anodic peak current detection. The amperometric signal of the redox probe increase with the H1N1 virus concentration.

4.4. HIV (Human Immunodeficiency Virus)

In the diagnosis of human immunodeficiency virus type 1 (HIV-1), the detection of p24 antigen (HIV p24) plays an important role. This capsid protein is detectable several days before the host generates the virus, as opposed to the detection of its antibodies, the target of the current diagnostic tests.

For this purpose, Gan et al. developed an immunosensor increasing the sensitivity of the corresponding ELISA method by 1000 times by anchoring more than 100 units of HRP and almost 15 molecules of secondary antibody on a dextrin amine skeleton copolymer (Ac) labeled with gold nanocolloids [122]. The complex (AuNPs/Ac-HRP-Ab_{II}) can give rise to the sandwich assay by interacting with the p24 antigen, bound by primary antibodies immobilized on MNPs. The immunocomplex, thus formed, was dropped on a screen-printed carbon electrode (SPCE) and retained by a magnet due to its paramagnetic features.

The oxidation of catechol by HRP took place on the copolymer in presence of H_2O_2 and provides the electrochemical signal. In this instance, the use of Fe_3O_4 nanoparticles will not only increase the surface area available for Ab loading but simplify the separation process thanks to the paramagnetic properties of the magnetic core. Furthermore, the signal amplification associated with the use of AuNPs and the high protein surface density, produce a 1000-fold increase in electrochemical sensor sensitivity when compared to the corresponding ELISA method.

5. Conclusions

In the last years, nanotechnologies and biotechnologies have progressively played a crucial role in the development of high performance affinity-based electrochemical biosensors. Several new approaches were setup, dealing with the production of new nanostructured materials for sensing devices modification. In particular, combined and hybrid nanostructures such as decorated–GN/GO/rGO MeNPs, QDs and multi MeNPs have gathered great interest, thanks to their unique synergistic properties. To this end, new synthetic routes were developed, providing immediate and simple use of these materials. In this paper, some of the most relevant examples of electrochemical immunosensors realized during the last ten years have been described. Both sandwich and label-free configurations were widely used, with optimal results in terms of LOD and linear ranges, showing how NMs allow an efficient miniaturization of the electrochemical recognition system with high sensitivity and stability.

Among the interesting developments that can be glimpsed for the future, the most promising concern the exploitation of the signal amplification made possible by nanostructured materials, which, considering the remarkable efficiency of these systems, is possible even in the presence of small quantities of the latter. This aspect is of great relevance given the development of POCTs, which are generally based on disposable systems and therefore imply that the sensitive part of the sensor can be mass-produced at low costs. In particular,

the most recent studies described herein aimed at screening emerging viruses suggest that POCT based on nanostructured materials and electrochemical transduction could be a useful tool for a rapid and early identification of SARS-CoV-2 for making a decisive contribution to the containment of the CoViD-19 pandemic.

Author Contributions: Conceptualization: F.M.; Investigation: R.Z., F.P., C.D.; Supervision F.M., R.A., G.F.; Writing—original draft: F.M., R.Z., F.P., C.D., R.A., G.F. Writing—review and editing: F.M. All authors have read and agreed to the published version of the manuscript.

Funding: This research received no external funding.

Institutional Review Board Statement: Not applicable.

Informed Consent Statement: Not applicable.

Data Availability Statement: The data used to support the findings of this study are available from the corresponding author upon request.

Conflicts of Interest: The authors declare no conflict of interest.

References

1. Justino, C.I.; Duarte, A.C.; Rocha-Santos, T.A. Chapter Three—Immunosensors in clinical laboratory diagnostics. In *Advances in Clinical Chemistry*; Makowski, C.C., Ed.; Elsevier: Amsterdam, The Netherlands, 2016; Volume 73, pp. 65–108. [CrossRef]
2. Králík, P.; Ricchi, M. A Basic Guide to Real Time PCR in Microbial Diagnostics: Definitions, Parameters, and Everything. *Front. Microbiol.* **2017**, *8*, 108. [CrossRef] [PubMed]
3. Mascini, M.; Tombelli, S. Biosensors for biomarkers in medical diagnostics. *Biomarkers* **2008**, *13*, 637–657. [CrossRef] [PubMed]
4. Mollarasouli, F.; Kurbanoglu, S.; Özkan, S.A. The Role of Electrochemical Immunosensors in Clinical Analysis. *Biosensors* **2019**, *9*, 86. [CrossRef] [PubMed]
5. Antiochia, R.; Favero, G.; Conti, M.E.; Mazzei, F.; Tortolini, C. Affinity-based biosensors for pathogenic bacteria detection. *Int. J. Environ. Technol. Manag.* **2015**, *18*, 185. [CrossRef]
6. Zhang, X.; Guo, Q.; Cui, D. Recent Advances in Nanotechnology Applied to Biosensors. *Sensors* **2009**, *9*, 1033–1053. [CrossRef]
7. Mokhtarzadeh, A.; Eivazzadeh-Keihan, R.; Pashazadeh, P.; Hejazi, M.; Gharaatifar, N.; Hasanzadeh, M.; Baradaran, B.; De La Guardia, M. Nanomaterial-based biosensors for detection of pathogenic virus. *TrAC Trends Anal. Chem.* **2017**, *97*, 445–457. [CrossRef] [PubMed]
8. Holzinger, M.; Le Goff, A.; Cosnier, S. Nanomaterials for biosensing applications: A review. *Front. Chem.* **2014**, *2*, 63. [CrossRef]
9. Sanvicens, N.; Pastells, C.; Pascual, N.; Marco, M.-P. Nanoparticle-based biosensors for detection of pathogenic bacteria. *TrAC Trends Anal. Chem.* **2009**, *28*, 1243–1252. [CrossRef]
10. Ju, H.; Zhang, X.; Wang, J. *Signal Amplification for Nanobiosensing: Principles, Development and Application*; Springer: New York, NY, USA, 2011; pp. 39–84. [CrossRef]
11. Lei, J.; Ju, H. Signal amplification using functional nanomaterials for biosensing. *Chem. Soc. Rev.* **2012**, *41*, 2122–2134. [CrossRef]
12. Lee, S.H.; Sung, J.H.; Park, T.H. Nanomaterial-Based Biosensor as an Emerging Tool for Biomedical Applications. *Ann. Biomed. Eng.* **2011**, *40*, 1384–1397. [CrossRef]
13. Singh, P.; Pandey, S.K.; Singh, J.; Srivastava, S.; Sachan, S.; Singh, S.K. Biomedical Perspective of Electrochemical Nanobiosensor. *Nano-Micro Lett.* **2016**, *8*, 193–203. [CrossRef] [PubMed]
14. Ghafar-Zadeh, E. Wireless Integrated Biosensors for Point-of-Care Diagnostic Applications. *Sensors* **2015**, *15*, 3236–3261. [CrossRef] [PubMed]
15. Lim, S.A.; Ahmed, M.U. Electrochemical immunosensors and their recent nanomaterial-based signal amplification strategies: A review. *RSC Adv.* **2016**, *6*, 24995–25014. [CrossRef]
16. Khashayar, P.; Amoabediny, G.; Larijani, B.; Hosseini, M.; Vanfleteren, J. Fabrication and Verification of Conjugated AuNP-Antibody Nanoprobe for Sensitivity Improvement in Electrochemical Biosensors. *Sci. Rep.* **2017**, *7*, 16070. [CrossRef] [PubMed]
17. Siti, R.M.; Khairunisak, A.R.; Aziz, A.A.; Noordin, R.; Makhsin, S.R.; Razak, K.A.; Rahmah, N. Study on Controlled Size, Shape and Dispersity of Gold Nanoparticles (AuNPs) Synthesized via Seeded-Growth Technique for Immunoassay Labeling. *Adv. Mater. Res.* **2011**, *364*, 504–509. [CrossRef]
18. Wang, X.; Mei, Z.; Wang, Y.; Tang, L. Comparison of four methods for the biofunctionalization of gold nanorods by the introduction of sulfhydryl groups to antibodies. *Beilstein J. Nanotechnol.* **2017**, *8*, 372–380. [CrossRef]
19. He, Q.; Zhu, Z.; Jin, L.; Peng, L.; Guo, W.; Hu, S. Detection of HIV-1 p24 antigen using streptavidin–biotin and gold nanoparticles based immunoassay by inductively coupled plasma mass spectrometry. *J. Anal. At. Spectrom.* **2014**, *29*, 1477–1482. [CrossRef]
20. Fan, Y.; Shi, S.; Ma, J.; Guo, Y. A paper-based electrochemical immunosensor with reduced graphene oxide/thionine/gold nanoparticles nanocomposites modification for the detection of cancer antigen 125. *Biosens. Bioelectron.* **2019**, *135*, 1–7. [CrossRef]

21. Ren, X.; Wu, D.; Wang, Y.; Zhang, Y.; Fan, D.; Pang, X.; Li, Y.; Du, B.; Wei, Q. An ultrasensitive squamous cell carcinoma antigen biosensing platform utilizing double-antibody single-channel amplification strategy. *Biosens. Bioelectron.* **2015**, *72*, 156–159. [CrossRef]
22. Qi, T.; Liao, J.; Li, Y.; Peng, J.; Li, W.; Chu, B.; Li, H.; Wei, Y.; Qiana, Z. Label-free alpha fetoprotein immunosensor established by the facile synthesis of a palladium–graphene nanocomposite. *Biosens. Bioelectron.* **2014**, *61*, 245–250. [CrossRef]
23. Suresh, L.; Bondili, J.S.; Brahman, P. Fabrication of Immunosensor Based on Polyaniline, Fullerene-C 60 and Palladium Nanoparticles Nanocomposite: An Electrochemical Detection Tool for Prostate Cancer. *Electroanalysis* **2020**, *32*, 1439–1448. [CrossRef]
24. Zheng, Y.; Wang, H.; Ma, Z. A nanocomposite containing Prussian Blue, platinum nanoparticles and polyaniline for multi-amplification of the signal of voltammetric immunosensors: Highly sensitive detection of carcinoma antigen 125. *Microchim. Acta* **2017**, *184*, 4269–4277. [CrossRef]
25. Lan, Q.; Ren, C.; Lambert, A.; Zhang, G.; Li, J.; Cheng, Q.; Hu, X.; Yang, Z. Platinum Nanoparticle-decorated Graphene Oxide@Polystyrene Nanospheres for Label-free Electrochemical Immunosensing of Tumor Markers. *ACS Sustain. Chem. Eng.* **2020**, *8*, 4392–4399. [CrossRef]
26. Piguillem, S.V.; Ortega, F.G.; Raba, J.; Messina, G.A.; Fernández-Baldo, M.A. Development of a nanostructured electrochemical immunosensor applied to the early detection of invasive aspergillosis. *Microchem. J.* **2018**, *139*, 394–400. [CrossRef]
27. Sureshab, L.; Bondili, J.; Brahman, P. Development of proof of concept for prostate cancer detection: An electrochemical immunosensor based on fullerene-C60 and copper nanoparticles composite film as diagnostic tool. *Mater. Today Chem.* **2020**, *16*, 100257. [CrossRef]
28. Upan, J.; Banet, P.; Aubert, P.-H.; Ounnunkad, K.; Jakmunee, J. Sequential injection-differential pulse voltammetric immunosensor for hepatitis B surface antigen using the modified screen-printed carbon electrode. *Electrochim. Acta* **2020**, *349*, 136335. [CrossRef]
29. Valipour, A.; Roushani, M. Fabrication of an electrochemical immunosensor for determination of human chorionic gonadotropin based on PtNPs/cysteamine/AgNPs as an efficient interface. *Anal. Bioanal. Chem. Res.* **2017**, *4*, 341–352. [CrossRef]
30. Cho, I.-H.; Lee, J.; Kim, J.; Kang, M.-S.; Paik, J.K.; Ku, S.; Cho, H.-M.; Irudayaraj, J.; Kim, D.-H. Current Technologies of Electrochemical Immunosensors: Perspective on Signal Amplification. *Sensors* **2018**, *18*, 207. [CrossRef]
31. Tang, J.; Tanga, D. Non-enzymatic electrochemical immunoassay using noble metal nanoparticles: A review. *Microchim. Acta* **2015**, *182*, 2077–2089. [CrossRef]
32. Doron, A.; Katz, E.; Willner, I. Organization of Au Colloids as Monolayer Films onto ITO Glass Surfaces: Application of the Metal Colloid Films as Base Interfaces To Construct Redox-Active Monolayers. *Langmuir* **1995**, *11*, 1313–1317. [CrossRef]
33. Iglesias-Mayor, A.; Amor-Gutiérrez, O.; Costa-García, A.; De La Escosura-Muñiz, A. Nanoparticles as Emerging Labels in Electrochemical Immunosensors. *Sensors* **2019**, *19*, 5137. [CrossRef] [PubMed]
34. Pang, P.; Teng, X.; Chen, M.; Zhang, Y.; Wang, H.; Yang, C.; Yangc, W.; Barrow, C.J. Ultrasensitive enzyme-free electrochemical immunosensor for microcystin-LR using molybdenum disulfide/gold nanoclusters nanocomposites as platform and Au@Pt core-shell nanoparticles as signal enhancer. *Sens. Actuators B Chem.* **2018**, *266*, 400–407. [CrossRef]
35. Li, N.; Ma, H.; Cao, W.; Wu, D.; Yan, T.; Du, B.; Wei, Q. Highly sensitive electrochemical immunosensor for the detection of alpha fetoprotein based on PdNi nanoparticles and N-doped graphene nanoribbons. *Biosens. Bioelectron.* **2015**, *74*, 786–791. [CrossRef] [PubMed]
36. Zhang, X.; Zhou, D.; Sheng, S.; Yang, J.; Chen, X.; Xie, G.; Xiang, H. Electrochemical immunoassay for the cancer marker LMP-1 (Epstein-Barr virus-derived latent membrane protein 1) using a glassy carbon electrode modified with Pd@Pt nanoparticles and a nanocomposite consisting of graphene sheets and MWCNTs. *Microchim. Acta* **2016**, *183*, 2055–2062. [CrossRef]
37. Zhang, J.; Xiong, Z.; Chen, Z. Ultrasensitive electrochemical microcystin-LR immunosensor using gold nanoparticle functional polypyrrole microsphere catalyzed silver deposition for signal amplification. *Sens. Actuators B Chem.* **2017**, *246*, 623–630. [CrossRef]
38. Ho, J.-A.A.; Chang, H.-C.; Shih, N.-Y.; Wu, L.-C.; Chang, Y.-F.; Chen, C.-C.; Chou, C. Diagnostic Detection of Human Lung Cancer-Associated Antigen Using a Gold Nanoparticle-Based Electrochemical Immunosensor. *Anal. Chem.* **2010**, *82*, 5944–5950. [CrossRef] [PubMed]
39. Huang, J.; Xie, Z.; Xie, Z.; Luo, S.; Xie, L.; Huang, L.; Fan, Q.; Zhang, Y.; Wang, S.; Zeng, T. Silver nanoparticles coated graphene electrochemical sensor for the ultrasensitive analysis of avian influenza virus H7. *Anal. Chim. Acta* **2016**, *913*, 121–127. [CrossRef]
40. Zhang, Z.; Yang, M.; Wu, X.; Dong, S.; Zhu, N.; Gyimah, E.; Wang, K.; Li, Y. A competitive immunosensor for ultrasensitive detection of sulphonamides from environmental waters using silver nanoparticles decorated single-walled carbon nanohorns as labels. *Chemosphere* **2019**, *225*, 282–287. [CrossRef]
41. Ning, S.; Zhou, M.; Liu, C.; Waterhouse, G.I.; Dong, J.; Ai, S. Ultrasensitive electrochemical immunosensor for avian leukosis virus detection based on a β-cyclodextrin-nanogold-ferrocene host-guest label for signal amplification. *Anal. Chim. Acta* **2019**, *1062*, 87–93. [CrossRef]
42. Alizadeh, N.; Hallaj, R.; Salimi, A. A highly sensitive electrochemical immunosensor for hepatitis B virus surface antigen detection based on Hemin/G-quadruplex horseradish peroxidase-mimicking DNAzyme-signal amplification. *Biosens. Bioelectron.* **2017**, *94*, 184–192. [CrossRef]
43. Fan, L.; Yan, Y.; Guoa, B.; Zhaoa, M.; Lia, J.; Biana, X.; Wua, H.; Cheng, W.; Ding, S. Trimetallic hybrid nanodendrites and magnetic nanocomposites-based electrochemical immunosensor for ultrasensitive detection of serum human epididymis protein 4. *Sens. Actuators B Chem.* **2019**, *296*, 126697. [CrossRef]

44. Azmi, U.Z.M.; Yusof, N.A.; Kusnin, N.; Abdullah, J.; Suraiya, S.; Ong, P.S.; Raston, N.H.A.; Rahman, S.F.A.; Fathil, M.F.M. Sandwich Electrochemical Immunosensor for Early Detection of Tuberculosis Based on Graphene/Polyaniline-Modified Screen-Printed Gold Electrode. *Sensors* **2018**, *18*, 3926. [CrossRef] [PubMed]
45. Valera, E.; Hernández-Albors, A.; Marco, M.-P. Electrochemical coding strategies using metallic nanoprobes for biosensing applications. *TrAC Trends Anal. Chem.* **2016**, *79*, 9–22. [CrossRef]
46. Maiti, D.; Tong, X.; Mou, X.; Yang, K. Carbon-Based Nanomaterials for Biomedical Applications: A Recent Study. *Front. Pharmacol.* **2019**, *9*, 1401. [CrossRef] [PubMed]
47. Heydari-Bafrooei, E.; Ensafi, A.A. *Typically Used Carbon-Based Nanomaterials in the Fabrication of Biosensors*; Elsevier: Amsterdam, The Netherlands, 2019; pp. 77–98. [CrossRef]
48. Ramnani, P.; Saucedo, N.M.; Mulchandani, A. Carbon nanomaterial-based electrochemical biosensors for label-free sensing of environmental pollutants. *Chemosphere* **2016**, *143*, 85–98. [CrossRef] [PubMed]
49. Shao, Y.; Wang, J.; Wu, H.; Liu, J.; Aksay, I.A.; Lin, Y. Graphene Based Electrochemical Sensors and Biosensors: A Review. *Electroanalysis* **2010**, *22*, 1027–1036. [CrossRef]
50. Crevillen, A.G.; Escarpa, A.; Garcia, C.D. *Chapter 1 Carbon-Based Nanomaterials in Analytical Chemistry*; Royal Society of Chemistry: London, UK, 2018; pp. 1–36. [CrossRef]
51. Amani, J.; Khoshroo, A.; Rahimi-Nasrabadi, M. Electrochemical immunosensor for the breast cancer marker CA 15–3 based on the catalytic activity of a CuS/reduced graphene oxide nanocomposite towards the electrooxidation of catechol. *Microchim. Acta* **2017**, *185*, 79. [CrossRef]
52. Barman, S.C.; Hossain, M.F.; Park, J.Y. Gold Nanoparticles Assembled Chemically Functionalized Reduced Graphene Oxide Supported Electrochemical Immunosensor for Ultra-Sensitive Prostate Cancer Detection. *J. Electrochem. Soc.* **2017**, *164*, B234–B239. [CrossRef]
53. Gao, Y.-S.; Zhu, X.-F.; Xu, J.; Lu, L.; Wang, W.-M.; Yang, T.-T.; Xing, H.-K.; Yu, Y.-F. Label-free electrochemical immunosensor based on Nile blue A-reduced graphene oxide nanocomposites for carcinoembryonic antigen detection. *Anal. Biochem.* **2016**, *500*, 80–87. [CrossRef]
54. Singh, R.; Hong, S.; Jang, J. Label-free Detection of Influenza Viruses using a Reduced Graphene Oxide-based Electrochemical Immunosensor Integrated with a Microfluidic Platform. *Sci. Rep.* **2017**, *7*, 42771. [CrossRef]
55. Singh, S.; Tuteja, S.K.; Sillu, D.; Deep, A.; Suri, C.R. Gold nanoparticles-reduced graphene oxide based electrochemical immunosensor for the cardiac biomarker myoglobin. *Microchim. Acta* **2016**, *183*, 1729–1738. [CrossRef]
56. Wang, R.; Feng, J.-J.; Xue, Y.; Wu, L.; Wang, A.-J. A label-free electrochemical immunosensor based on AgPt nanorings supported on reduced graphene oxide for ultrasensitive analysis of tumor marker. *Sens. Actuators B Chem.* **2018**, *254*, 1174–1181. [CrossRef]
57. Li, J.; Liu, S.; Yu, J.; Lian, W.; Cui, M.; Xu, W.; Huang, J. Electrochemical immunosensor based on graphene–polyaniline composites and carboxylated graphene oxide for estradiol detection. *Sens. Actuators B Chem.* **2013**, *188*, 99–105. [CrossRef]
58. Loo, A.H.; Ambrosi, A.; Bonanni, A.; Pumera, M. CVD graphene based immunosensor. *RSC Adv.* **2014**, *4*, 23952–23956. [CrossRef]
59. Hong, C.; Qiao, X.; Wang, H.; Sun, Z.; Qi, Y.; Hong, C. An electrochemical immunosensor for simultaneous point-of-care cancer markers based on the host–guest inclusion of β-cyclodextrin–graphene oxide. *J. Mater. Chem. B* **2016**, *4*, 990–996. [CrossRef]
60. Lai, G.; Cheng, H.; Xin, D.; Zhang, H.; Yu, A. Amplified inhibition of the electrochemical signal of ferrocene by enzyme-functionalized graphene oxide nanoprobe for ultrasensitive immunoassay. *Anal. Chim. Acta* **2016**, *902*, 189–195. [CrossRef]
61. Yáñez-Sedeño, P.; González-Cortés, A.; Agüí, L.; Pingarrón, J.M. Uncommon Carbon Nanostructures for the Preparation of Electrochemical Immunosensors. *Electroanalysis* **2016**, *28*, 1679–1691. [CrossRef]
62. Serafín, V.; Valverde, A.; Martínez-García, G.; Martínez-Periñán, E.; Comba, F.; Garranzo-Asensio, M.; Barderas, R.; Yáñez-Sedeño, P.; Campuzano, S.; Pingarrón, J. Graphene quantum dots-functionalized multi-walled carbon nanotubes as nanocarriers in electrochemical immunosensing. Determination of IL-13 receptor α2 in colorectal cells and tumor tissues with different metastatic potential. *Sens. Actuators B Chem.* **2019**, *284*, 711–722. [CrossRef]
63. Luo, Y.; Wang, Y.; Yan, H.; Wu, Y.; Zhu, C.; Du, D.; Lin, Y. SWCNTs@GQDs composites as nanocarriers for enzyme-free dual-signal amplification electrochemical immunoassay of cancer biomarker. *Anal. Chim. Acta* **2018**, *1042*, 44–51. [CrossRef]
64. Asadian, E.; Ghalkhani, M.; Shahrokhianab, S. Electrochemical sensing based on carbon nanoparticles: A review. *Sens. Actuators B Chem.* **2019**, *293*, 183–209. [CrossRef]
65. Cheng, Z.X.; Ang, W.L.; Bonanni, A. Electroactive Nanocarbon Can Simultaneously Work as Platform and Signal Generator for Label-Free Immunosensing. *ChemElectroChem* **2019**, *6*, 3615–3620. [CrossRef]
66. Allen, B.L.; Kichambare, P.D.; Star, A. Carbon Nanotube Field-Effect-Transistor-Based Biosensors. *Adv. Mater.* **2007**, *19*, 1439–1451. [CrossRef]
67. Kim, S.N.; Rusling, J.F.; Papadimitrakopoulos, F. Carbon Nanotubes for Electronic and Electrochemical Detection of Biomolecules. *Adv. Mater.* **2007**, *19*, 3214–3228. [CrossRef] [PubMed]
68. Bhardwaj, J.; Devarakonda, S.; Kumar, S.; Jang, J. Development of a paper-based electrochemical immunosensor using an antibody-single walled carbon nanotubes bio-conjugate modified electrode for label-free detection of foodborne pathogens. *Sens. Actuators B Chem.* **2017**, *253*, 115–123. [CrossRef]
69. Cabral, D.G.; Lima, E.C.; Moura, P.; Dutra, R.A.F. A label-free electrochemical immunosensor for hepatitis B based on hyaluronic acid–carbon nanotube hybrid film. *Talanta* **2016**, *148*, 209–215. [CrossRef]

70. Huang, K.; Niu, D.-J.; Xie, W.-Z.; Wang, W. A disposable electrochemical immunosensor for carcinoembryonic antigen based on nano-Au/multi-walled carbon nanotubes–chitosans nanocomposite film modified glassy carbon electrode. *Anal. Chim. Acta* **2010**, *659*, 102–108. [CrossRef]
71. Malhotra, R.; Patel, V.; Vaqué, J.P.; Gutkind, J.S.; Rusling, J.F. Ultrasensitive Electrochemical Immunosensor for Oral Cancer Biomarker IL-6 Using Carbon Nanotube Forest Electrodes and Multilabel Amplification. *Anal. Chem.* **2010**, *82*, 3118–3123. [CrossRef]
72. Sánchez-Tirado, E.; Salvo, C.; González-Cortés, A.; Yáñez-Sedeño, P.; Langa, F.; Pingarrón, J. Electrochemical immunosensor for simultaneous determination of interleukin-1 beta and tumor necrosis factor alpha in serum and saliva using dual screen printed electrodes modified with functionalized double–walled carbon nanotubes. *Anal. Chim. Acta* **2017**, *959*, 66–73. [CrossRef] [PubMed]
73. Valverde, A.; Serafín, V.; Montero-Calle, A.; González-Cortés, A.; Barderas, R.; Yáñez-Sedeño, P.; Campuzano, S.; Pingarrón, J.M. Carbon/Inorganic Hybrid Nanoarchitectures as Carriers for Signaling Elements in Electrochemical Immunosensors: First Biosensor for the Determination of the Inflammatory and Metastatic Processes Biomarker RANK-ligand. *ChemElectroChem* **2020**, *7*, 810–820. [CrossRef]
74. Serafín, V.; Valverde, A.; Garranzo-Asensio, M.; Barderas, R.; Campuzano, S.; Yáñez-Sedeño, P.; Pingarrón, J.M. Simultaneous amperometric immunosensing of the metastasis-related biomarkers IL-13Rα2 and CDH-17 by using grafted screen-printed electrodes and a composite prepared from quantum dots and carbon nanotubes for signal amplification. *Microchim. Acta* **2019**, *186*, 411. [CrossRef]
75. Pumera, M. Electrochemistry of graphene: New horizons for sensing and energy storage. *Chem. Rec.* **2009**, *9*, 211–223. [CrossRef] [PubMed]
76. Huang, W.; Xiang, G.; Jiang, D.; Liu, L.; Liu, C.; Liu, F.; Pu, X.; And, F.L. Electrochemical Immunoassay forCytomegalovirusAntigen Detection with Multiple Signal Amplification Using HRP and Pt-Pd Nanoparticles Functionalized Single-walled Carbon Nanohorns. *Electroanalysis* **2016**, *28*, 1126–1133. [CrossRef]
77. Tirado, E.S.; Cortés, A.G.; Yudasaka, M.; Iijima, S.; Langa, F.; Sedeño, P.Y.; Pingarrón, J. Electrochemical immunosensor for the determination of 8-isoprostane aging biomarker using carbon nanohorns-modified disposable electrodes. *J. Electroanal. Chem.* **2017**, *793*, 197–202. [CrossRef]
78. Gao, Z. Electrochemical Immunosensor for Monocyte Chemoattractant Protein-1 Detection Based on Pt Nanoparticles Functionalized Single-walled Carbon Nanohorns. *Int. J. Electrochem. Sci.* **2018**, *13*, 3923–3934. [CrossRef]
79. Yang, M.; Wu, X.; Hu, X.-L.; Wang, K.; Zhang, C.; Gyimah, E.; Yakubu, S.; Zhang, Z. Electrochemical immunosensor based on Ag+-dependent CTAB-AuNPs for ultrasensitive detection of sulfamethazine. *Biosens. Bioelectron.* **2019**, *144*, 111643. [CrossRef]
80. Yang, F.; Han, J.; Zhuo, Y.; Yang, Z.; Chai, Y.-Q.; Yuan, R. Highly sensitive impedimetric immunosensor based on single-walled carbon nanohorns as labels and bienzyme biocatalyzed precipitation as enhancer for cancer biomarker detection. *Biosens. Bioelectron.* **2014**, *55*, 360–365. [CrossRef] [PubMed]
81. Liu, F.; Xiang, G.; Yuan, R.; Chen, X.; Luo, F.; Jiang, D.; Huang, S.; Li, Y.; Pu, X. Procalcitonin sensitive detection based on graphene–gold nanocomposite film sensor platform and single-walled carbon nanohorns/hollow Pt chains complex as signal tags. *Biosens. Bioelectron.* **2014**, *60*, 210–217. [CrossRef]
82. Pilehvar, S.; De Wael, K. Recent Advances in Electrochemical Biosensors Based on Fullerene-C60 Nano-Structured Platforms. *Biosensors* **2015**, *5*, 712–735. [CrossRef]
83. Hirsch, A. Functionalization of fullerenes and carbon nanotubes. *Phys. Status Solidi* **2006**, *243*, 3209–3212. [CrossRef]
84. Demirbakan, B.; Sezgintürk, M.K. A novel immunosensor based on fullerene C60 for electrochemical analysis of heat shock protein 70. *J. Electroanal. Chem.* **2016**, *783*, 201–207. [CrossRef]
85. Li, Y.; Fang, L.; Cheng, P.; Deng, J.; Jiang, L.; Huang, H.; Zheng, J. An electrochemical immunosensor for sensitive detection of Escherichia coli O157:H7 using C60 based biocompatible platform and enzyme functionalized Pt nanochains tracing tag. *Biosens. Bioelectron.* **2013**, *49*, 485–491. [CrossRef] [PubMed]
86. Sun, X.; Li, Z.; Cai, Y.; Wei, Z.; Fang, Y.; Ren, G.; Huang, Y. Electrochemical impedance spectroscopy for analytical determination of paraquat in meconium samples using an immunosensor modified with fullerene, ferrocene and ionic liquid. *Electrochim. Acta* **2011**, *56*, 1117–1122. [CrossRef]
87. Mazloum-Ardakani, M.; Hosseinzadeh, L.; Khoshroo, A. Label-free electrochemical immunosensor for detection of tumor necrosis factor α based on fullerene-functionalized carbon nanotubes/ionic liquid. *J. Electroanal. Chem.* **2015**, *757*, 58–64. [CrossRef]
88. Zhang, W.; Patel, K.; Schexnider, A.; Banu, S.; Radadia, A.D. Nanostructuring of Biosensing Electrodes with Nanodiamonds for Antibody Immobilization. *ACS Nano* **2014**, *8*, 1419–1428. [CrossRef]
89. Pashchenko, O.; Shelby, T.; Banerjee, T.; Santra, S. A Comparison of Optical, Electrochemical, Magnetic, and Colorimetric Point-of-Care Biosensors for Infectious Disease Diagnosis. *ACS Infect. Dis.* **2018**, *4*, 1162–1178. [CrossRef] [PubMed]
90. Beitollahi, H.; Khalilzadeh, M.A.; Tajik, S.; Safaei, M.; Zhang, K.; Jang, H.W.; Shokouhimehr, M. Recent Advances in Applications of Voltammetric Sensors Modified with Ferrocene and Its Derivatives. *ACS Omega* **2020**, *5*, 2049–2059. [CrossRef]
91. Singh, S.; Nagpal, M.; Singh, P.; Chauhan, P.; Zaidi, M.A. Tumor markers: A diagnostic tool. *Natl. J. Maxillofac. Surg.* **2016**, *7*, 17–20. [CrossRef] [PubMed]
92. Kumar, S.; Mohan, A.; Guleria, R. Biomarkers in cancer screening, research and detection: Present and future: A review. *Biomarkers* **2006**, *11*, 385–405. [CrossRef]

93. Wu, J.; Fu, Z.; Yan, F.; Ju, H. Biomedical and clinical applications of immunoassays and immunosensors for tumor markers. *TrAC Trends Anal. Chem.* **2007**, *26*, 679–688. [CrossRef]
94. Filik, H.; Avan, A.A. Nanostructures for nonlabeled and labeled electrochemical immunosensors: Simultaneous electrochemical detection of cancer markers: A review. *Talanta* **2019**, *205*, 120153. [CrossRef]
95. Kufe, D. Mucins in cancer: Function, prognosis and therapy. *Nat. Rev. Cancer* **2009**, *9*, 874–885. [CrossRef] [PubMed]
96. Rittenhouse, H.G.; Manderino, G.L.; Hass, G.M. Mucin-Type Glycoproteins as Tumor Markers. *Lab. Med.* **1985**, *16*, 556–560. [CrossRef]
97. Chauhan, S.C.; Kumar, D.; Jaggi, M. Mucins in ovarian cancer diagnosis and therapy. *J. Ovarian Res.* **2009**, *2*, 21. [CrossRef] [PubMed]
98. Chikkaveeraiah, B.V.; Bhirde, A.A.; Morgan, N.Y.; Eden, H.S.; Chen, X. Electrochemical Immunosensors for Detection of Cancer Protein Biomarkers. *ACS Nano* **2012**, *6*, 6546–6561. [CrossRef] [PubMed]
99. Chao, A.; Tang, Y.-H.; Lai, C.; Chang, C.-J.; Chang, S.-C.; Wu, T.-I.; Hsueh, S.; Wang, C.-J.; Chou, H.-H.; Chang, T.-C. Potential of an age-stratified CA125 cut-off value to improve the prognostic classification of patients with endometrial cancer. *Gynecol. Oncol.* **2013**, *129*, 500–504. [CrossRef] [PubMed]
100. Kumar, N.; Sharma, S.; Nara, S. Dual gold nanostructure-based electrochemical immunosensor for CA125 detection. *Appl. Nanosci.* **2018**, *8*, 1843–1853. [CrossRef]
101. Pakchinab, P.; Fathib, M.; Ghanbaria, H.; Saber, R.; Omidi, Y. A novel electrochemical immunosensor for ultrasensitive detection of CA125 in ovarian cancer. *Biosens. Bioelectron.* **2020**, *153*, 112029. [CrossRef]
102. Reijnen, C.; Visser, N.C.M.; Kasius, J.C.; Boll, D.; Geomini, P.M.; Ngo, H.; Van Hamont, D.; Pijlman, B.M.; Vos, M.C.; Bulten, J.; et al. Improved preoperative risk stratification with CA-125 in low-grade endometrial cancer: A multicenter prospective cohort study. *J. Gynecol. Oncol.* **2019**, *30*, e70. [CrossRef]
103. Huang, Z.; Jiang, Z.; Zhao, C.; Han, W.; Lin, L.; Liu, A.; Weng, S.; Lin, X. Simple and effective label-free electrochemical immunoassay for carbohydrate antigen 19-9 based on polythionine-Au composites as enhanced sensing signals for detecting different clinical samples. *Int. J. Nanomed.* **2017**, *12*, 3049–3058. [CrossRef]
104. Imaoka, H.; Shimizu, Y.; Senda, Y.; Natsume, S.; Mizuno, N.; Hara, K.; Hijioka, S.; Hieda, N.; Tajika, M.; Tanaka, T.; et al. Post-adjuvant chemotherapy CA19-9 levels predict prognosis in patients with pancreatic ductal adenocarcinoma: A retrospective cohort study. *Pancreatology* **2016**, *16*, 658–664. [CrossRef]
105. Stieber, P.; Nagel, R.; Blankenburg, I.; Heinemann, V.; Untch, M.; Bauerfeind, I.; Di Gioia, D. Diagnostic efficacy of CA 15-3 and CEA in the early detection of metastatic breast cancer—A retrospective analysis of kinetics on 743 breast cancer patients. *Clin. Chim. Acta* **2015**, *448*, 228–231. [CrossRef] [PubMed]
106. Ge, S.; Jiao, X.; Chen, D. Ultrasensitive electrochemical immunosensor for CA 15-3 using thionine-nanoporous gold-graphene as a platform and horseradish peroxidase-encapsulated liposomes as signal amplification. *Analyst* **2012**, *137*, 4440–4447. [CrossRef] [PubMed]
107. Gui, J.-C.; Yan, W.-L.; Liu, X. CA19-9 and CA242 as tumor markers for the diagnosis of pancreatic cancer: A meta-analysis. *Clin. Exp. Med.* **2013**, *14*, 225–233. [CrossRef] [PubMed]
108. Du, X.; Zheng, X.; Zhang, Z.; Wu, X.; Sun, L.; Zhou, J.; Liu, M. A Label-Free Electrochemical Immunosensor for Detection of the Tumor Marker CA242 Based on Reduced Graphene Oxide-Gold-Palladium Nanocomposite. *Nanomaterials* **2019**, *9*, 1335. [CrossRef]
109. George, S.M.; Tandon, S.; Kandasubramanian, B. Advancements in Hydrogel-Functionalized Immunosensing Platforms. *ACS Omega* **2020**, *5*, 2060–2068. [CrossRef]
110. Tang, Z.; Fu, Y.; Ma, Z. Multiple signal amplification strategies for ultrasensitive label-free electrochemical immunoassay for carbohydrate antigen 24-2 based on redox hydrogel. *Biosens. Bioelectron.* **2017**, *91*, 299–305. [CrossRef]
111. Wang, Y.; Zhao, G.; Zhang, Y.; Pang, X.; Cao, W.; Du, B.; Wei, Q. Sandwich-type electrochemical immunosensor for CEA detection based on Ag/MoS_2@Fe_3O_4 and an analogous ELISA method with total internal reflection microscopy. *Sens. Actuators B Chem.* **2018**, *266*, 561–569. [CrossRef]
112. Zhao, C.; Ma, C.; Wu, M.; Li, W.; Song, Y.; Hong, C.; Qiao, X. A novel electrochemical immunosensor based on CoS2 for early screening of tumor marker carcinoembryonic antigen. *New J. Chem.* **2020**, *44*, 3524–3532. [CrossRef]
113. Idris, A.O.; Mabuba, N.; Arotiba, O.A. An Exfoliated Graphite-Based Electrochemical Immunosensor on a Dendrimer/Carbon Nanodot Platform for the Detection of Carcinoembryonic Antigen Cancer Biomarker. *Biosensors* **2019**, *9*, 39. [CrossRef]
114. Wei, Q.; Wang, Y.; Cao, W.; Zhang, Y.; Yan, T.; Du, B.; Wei, Q. An ultrasensitive electrochemical immunosensor for CEA using MWCNT-NH2 supported PdPt nanocages as labels for signal amplification. *J. Mater. Chem. B* **2015**, *3*, 2006–2011. [CrossRef]
115. Galle, P.; Foerster, F.; Kudo, M.; Chan, S.L.; Llovet, J.M.; Qin, S.; Schelman, W.R.; Chintharlapalli, S.; Abada, P.B.; Sherman, M.; et al. Biology and significance of alpha-fetoprotein in hepatocellular carcinoma. *Liver Int.* **2019**, *39*, 2214–2229. [CrossRef] [PubMed]
116. Jiao, L.; Mu, Z.; Zhu, C.; Wei, Q.; Li, H.; Du, D.; Lin, Y. Graphene loaded bimetallic Au@Pt nanodendrites enhancing ultrasensitive electrochemical immunoassay of AFP. *Sens. Actuators B Chem.* **2016**, *231*, 513–519. [CrossRef]
117. Liu, Q.; Yang, T.; Ye, Y.; Chen, P.; Ren, X.-N.; Rao, A.; Wan, Y.; Wang, B.; Luo, Z. A highly sensitive label-free electrochemical immunosensor based on an aligned GaN nanowires array/polydopamine heterointerface modified with Au nanoparticles. *J. Mater. Chem. B* **2019**, *7*, 1442–1449. [CrossRef] [PubMed]

118. Nayak, S.; Blumenfeld, N.R.; Laksanasopin, T.; Sia, S.K. Point-of-Care Diagnostics: Recent Developments in a Connected Age. *Anal. Chem.* **2017**, *89*, 102–123. [CrossRef] [PubMed]
119. LaFleur, J.P.; Jönsson, A.; Senkbeil, S.; Kutter, J.P. Recent advances in lab-on-a-chip for biosensing applications. *Biosens. Bioelectron.* **2016**, *76*, 213–233. [CrossRef] [PubMed]
120. Seo, G.; Lee, G.; Kim, M.J.; Baek, S.-H.; Choi, M.; Ku, K.B.; Lee, C.-S.; Jun, S.; Park, D.; Kim, H.G.; et al. Rapid Detection of COVID-19 Causative Virus (SARS-CoV-2) in Human Nasopharyngeal Swab Specimens Using Field-Effect Transistor-Based Biosensor. *ACS Nano* **2020**, *14*, 5135–5142. [CrossRef]
121. Fabiani, L.; Saroglia, M.; Galatà, G.; De Santis, R.; Fillo, S.; Luca, V.; Faggioni, G.; D'Amore, N.; Regalbuto, E.; Salvatori, P.; et al. Magnetic beads combined with carbon black-based screen-printed electrodes for COVID-19: A reliable and miniaturized electrochemical immunosensor for SARS-CoV-2 detection in saliva. *Biosens. Bioelectron.* **2021**, *171*, 112686. [CrossRef]
122. Gan, N.; Du, X.; Cao, Y.; Hu, F.; Lia, T.; Jiang, Q.-L. An Ultrasensitive Electrochemical Immunosensor for HIV p24 Based on Fe_3O_4@SiO_2 Nanomagnetic Probes and Nanogold Colloid-Labeled Enzyme–Antibody Copolymer as Signal Tag. *Materials* **2013**, *6*, 1255–1269. [CrossRef]
123. Ding, C.; Li, H.; Hu, K.; Lin, J.-M. Electrochemical immunoassay of hepatitis B surface antigen by the amplification of gold nanoparticles based on the nanoporous gold electrode. *Talanta* **2010**, *80*, 1385–1391. [CrossRef]
124. Shen, G.; Zhang, Y. Highly sensitive electrochemical stripping detection of hepatitis B surface antigen based on copper-enhanced gold nanoparticle tags and magnetic nanoparticles. *Anal. Chim. Acta* **2010**, *674*, 27–31. [CrossRef]
125. Wei, S.; Xiao, H.; Cao, L.; Chen, Z. A Label-Free Immunosensor Based on Graphene Oxide/Fe_3O_4/Prussian Blue Nanocomposites for the Electrochemical Determination of HBsAg. *Biosensors* **2020**, *10*, 24. [CrossRef] [PubMed]
126. Layqah, L.A.; Eissa, S. An electrochemical immunosensor for the corona virus associated with the Middle East respiratory syndrome using an array of gold nanoparticle-modified carbon electrodes. *Microchim. Acta* **2019**, *186*, 224. [CrossRef] [PubMed]
127. Zong, C.; Wu, J.; Xu, J.; Ju, H.; Yan, F. Multilayer hemin/G-quadruplex wrapped gold nanoparticles as tag for ultrasensitive multiplex immunoassay by chemiluminescence imaging. *Biosens. Bioelectron.* **2013**, *43*, 372–378. [CrossRef] [PubMed]
128. Mao, X.; Jiang, J.-H.; Luo, Y.; Shen, G.; Yu, R. Copper-enhanced gold nanoparticle tags for electrochemical stripping detection of human IgG. *Talanta* **2007**, *73*, 420–424. [CrossRef]
129. Yin, Y.; Wunderink, R.G. MERS, SARS and other coronaviruses as causes of pneumonia. *Respirology* **2017**, *23*, 130–137. [CrossRef]